ACS Catalysis

pubs.acs.org/acscatalysis Research Article

Selective Ethylbenzene Dehydrogenation to Styrene at Lewis Acid–Base Site Pairs on Zirconia Surfaces

Mikalai A. Artsiusheuski, Nicholas R. Jaegers, Carlos Lizandara-Pueyo, and Enrique Iglesia*

Cite This: ACS Catal. 2025, 15, 19102–19110 Read Online

ACCESS | Metrics & More | Article Recommendations | Supporting Information

ABSTRACT: The chemical dehydroxylation of monoclinic zirconia (m-ZrO_2) surfaces uncovers low-coordination Lewis acid–base (LAB) Zr–O pairs with very high reactivity and selectivity in nonoxidative ethylbenzene dehydrogenation to styrene and its reverse reactions (styrene hydrogenation). Ethylbenzene dehydrogenation rates (per mass) on dehydroxylated m-ZrO_2 significantly exceed those on promoted Fe-based catalysts, with selectivities above 95%. Kinetic trends for dehydrogenation and hydrogenation reactions reflect their respective stoichiometries, indicating that both reactions are mediated by the same kinetically relevant step on essentially bare LAB pairs. These mechanistic features lead to ratios of their respective rate constants given by the equilibrium constant for the overall reaction. The titration of LAB pairs by H_2O impurities in reactant streams leads to rates that decrease with time during the reaction; such rate losses can be reversed by periodic chemical dehydroxylation treatments and minimized by thorough purification of inlet streams. Dehydrogenation rates ultimately reached asymptotic values set by the relative rates of titration by H_2O and its removal by its reaction with ethylbenzene; such inherent chemical dehydroxylation reactions lead to essentially constant asymptotic rates. The uncovering and reactivity of LAB pairs at ZrO_2 surfaces render such solids (and related oxides) an attractive and unrecognized alternative to catalysts in current practice.

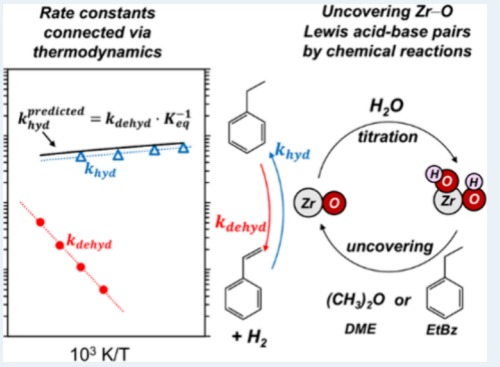

KEYWORDS: *dehydrogenation, ethylbenzene, earth-abundant oxides, Lewis acid–base pairs, ZrO_2, De Donder, kinetic modeling, site titration*

1. INTRODUCTION

Styrene is an intermediate in the synthesis of polymers; it is derived from ethylbenzene[1−4] via catalytic dehydrogenation processes, typically on Fe-based catalysts. This endothermic reaction requires high temperatures (823–873 K) and low pressures (<10 kPa) in order to overcome unfavorable thermodynamics. Steam is used as a gaseous diluent to achieve subambient pressures and to inhibit deactivation; its high heat capacity also makes it useful to limit the temperature drop in adiabatic reactors. The generation, condensation, and recycling of steam lead to second-law inefficiencies and to significant capital and operating costs.[5,6] The most competent catalysts are Fe-based, typically with chemical and structural promoters (Cr[1], Ce,[7,8] Mo[9,10]) that introduce cost, instability, and toxicity concerns. Styrene selectivities are high (90–97%), but exocyclic C–C cleavage reactions lead to some yield losses.[1,3,10] These challenges have led to the persistent search for steam-free processes, simpler catalyst formulations, and higher styrene yields and selectivities.[11−14]

Nonreducible oxides, such as monoclinic ZrO_2 (m-ZrO_2), catalyze nonoxidative dehydrogenation of acyclic and cyclic alkanes with high selectivity at gravimetric rates that are similar, and typically higher, than on dispersed metal nanoparticles and Cr-oxide domains in current use.[15−18] Dehydrogenation turnovers involve Zr–O Lewis acid–base (LAB) pairs exposed at ZrO_2 surfaces, which mediate the heterolytic cleavage of C–H bonds in kinetically relevant steps.[17] LAB pairs also catalyze aldol condensation and Meerwein–Ponndorf–Verley reactions.[19,20] The low-coordination features that are particularly effective at catalyzing these dehydrogenation and hydrogenation reactions are likely LAB site pairs located on steps, edges, and high-index facets, as supported by previous studies.[17,18] These Zr–O pairs, which stabilize C–H cleavage transition states (TS) also dissociate H_2O (during catalyst synthesis and exposure to ambient air), leading to strongly bound H (at O atoms) and OH (at the Zr atoms); these titrants render the most competent low-coordination sites inaccessible for catalytic turnovers.

The removal of bound H_2O (and CO_2) by thermal desorption requires temperatures that decrease surface areas and anneal the requisite low-coordination Zr–O site pairs.

Received: July 15, 2025
Revised: September 15, 2025
Accepted: October 24, 2025
Published: November 4, 2025

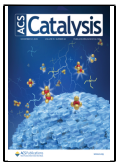

https://doi.org/10.1021/acscatal.5c04904
ACS Catal. 2025, 15, 19102–19110

Recently developed chemical treatment protocols allow the removal of these titrants at much lower temperatures, thus avoiding the loss of active sites inherent in desorptive treatments that require higher temperatures.[21−23] The sites uncovered by these chemical treatments must be kept from contact with titrants during catalysis, thus requiring strictly anhydrous and anaerobic reactant streams (O_2 forms H_2O and CO_2 during dehydrogenation reactions). In one embodiment, chemical dehydroxylation (and decarboxylation) of oxide surfaces with dimethyl ether (DME) forms CH_3OH, H_2, and CO via reactions with bound H−OH pairs at moderate temperatures (500−723 K); these DME treatments uncover the most competent Zr−O sites on *m*-ZrO_2 and lead to 60−120-fold rate enhancements (compared with samples thermally treated at 723 K) and very high selectivities (>99%) in dehydrogenation reactions of C_2−C_4 *n*-alkanes.[17,24]

This study describes the properties of LAB pairs uncovered by DME chemical treatments in the dehydrogenation of ethylbenzene to styrene. Reaction rates, kinetic trends, and elementary steps for this reaction and for its reverse (styrene hydrogenation) are reported here and compared with the rates for ethane dehydrogenation and ethene hydrogenation reactions. Chemical DME treatments at 723 K give higher rates for both ethylbenzene dehydrogenation and styrene hydrogenation (by factors of 62 and 50, respectively) than thermal treatments, consistent with the involvement of the same low-coordination LAB pairs in both reactions. The rate enhancements conferred by chemical treatments are also similar to those observed for C_2H_6 dehydrogenation (74-fold) and C_2H_4 hydrogenation (82-fold) at 773 K. Ethylbenzene dehydrogenation rates (per mass) on *m*-ZrO_2 catalysts are similar, or even higher, than on state-of-the-art reported catalysts. Styrene selectivities are greater than 95%, making these earth-abundant oxides attractive for steam-free non-oxidative styrene production. Equimolar amounts of methane and toluene (and ethane and benzene) were detected as the only trace products. Styrene-H_2 reactions form only ethylbenzene, indicative of the ability of these LAB pairs to saturate C=C double bonds in the side chains, but not within aromatic rings. Kinetic trends with reactants and products pressures for ethylbenzene dehydrogenation and styrene hydrogenation reflect their respective reaction stoichiometries, consistent with C−H activation steps at Zr−O pairs that remain essentially uncovered by reactive or spectator species during catalysis. The rates of hydrogenation and dehydrogenation at all pressures and temperatures are related to the thermodynamics of the interconversion of ethylbenzene, styrene, and H_2, an observation that requires, in turn, that dehydrogenation and hydrogenation turnovers occur via the same kinetically relevant transition state (TS), albeit in opposite directions.

The traces of H_2O that titrate the most competent LAB site pairs at *m*-ZrO_2 surfaces during the reaction gradually reverse the effects of chemical treatments on ethylbenzene dehydrogenation rates, but initial rates can be fully restored by subsequent DME treatments. Ethylbenzene reactants also act as surface dehydroxylation reagents during catalysis, leading to a balance between the rates of site titration by H_2O molecules in reactant streams and those of the scavenging of bound H_2O by ethylbenzene; this balance leads, in turn, to asymptotic ethylbenzene dehydrogenation rates after an initial period of reaction time and to constant rates thereafter.

2. METHODS

2.1. Catalyst Synthesis. Monoclinic zirconium dioxide catalysts (*m*-ZrO_2) were synthesized by the hydrothermal method. Separate solutions of 12.6 g of zirconyl nitrate ($ZrO(NO_3)_2$, Fisher Scientific, 99%) and 21.6 g of urea ($CO(NH_2)_2$, Sigma-Aldrich, 99.5%) were prepared each in 30 cm^3 of deionized H_2O (18.2 MΩ-cm) at 323 K. Afterward, solutions were mixed and transferred into a Teflon-lined autoclave, which was sealed and kept at 393 K for 20 h. The formed precipitates were suspended in deionized H_2O (18.2 MΩ·cm) and centrifuged at 8000 rpm, procedure was repeated four times. Powders were then dried in ambient stagnant air at 393 K for 12 h. Dried samples were treated in flowing He (Praxair, 99.999%, 2 $cm^3\ g^{-1}\ s^{-1}$) at 723 K (0.2 K s^{-1}) for 5 h. Treated powders were pressed (0.5 metric tons) and sieved to obtain 0.25−0.425 mm aggregates.

2.2. Chemical Treatments and Alkane Dehydrogenation Rate Measurements. Ethylbenzene dehydrogenation and styrene hydrogenation reactions on *m*-ZrO_2 catalysts were carried out in a straight quartz tubular reactor (9 mm inner diameter, 1.5 mm wall thickness). Catalyst aggregates (0.02 g) were mixed with quartz powder (1 g, Sigma-Aldrich, 0.18−0.25 mm; pretreated in 1 M HNO_3 at 293 K for 1 h, washed with 18.2 MΩ-cm H_2O, and then heated to 1073 K in flowing dry air at 10 K min^{-1} and held for 8 h). Catalyst−quartz mixtures were placed in the center of the reactor between quartz wool plugs. The reactor containing catalyst samples was heated using an Applied Test Systems 3210 series furnace. Temperatures were set by a Watlow 96 controller and measured using a K-type thermocouple, which was placed in contact with the outer reactor wall in the middle of the catalyst bed. Flows of gases were controlled using electronic mass flow controllers (Porter).

Catalysts were pretreated in a flow of He (Praxair, 99.999%; 40 $cm^3\ g^{-1}\ min^{-1}$) by heating to 723 K at 0.5 K s^{-1} and holding at this temperature for 1 h. Chemical cleaning protocols were applied as an activation step before the reaction. These treatments involved exposing the *m*-ZrO_2 catalyst to flow containing dimethyl ether (DME; 1.5 kPa; from Praxair, 5.0% DME, 5.0% Ar in He; 40 $cm^3\ g^{-1}\ s^{-1}$) for 0.25 h at 723 K and then to He flow for 0.5 h to remove residual DME and reaction products. Rate and selectivity measurements were carried out by flowing gas flows containing He, H_2 (Praxair, 99.999%), and ethylbenzene or styrene through the catalyst bed. Unless otherwise specified, He and H_2 reactant mixtures were additionally purified by flowing through an O_2/H_2O scrubber (Agilent 5182-9401, 5 ppb). Ethylbenzene (Sigma-Aldrich, 99.5+%) was used either as-supplied (referred to as "nonpurified"), additionally purified by contact with freshly calcined (723 K, 12 h) 4A molecular sieves (referred to as "purified"), or rigorously purified by refluxing over freshly calcined (773 K, 12 h) CBV720 molecular sieves and afterward dried by two consecutive treatments with freshly calcined (723 K, 12 h) 4A molecular sieves (referred to as "rigorously purified"). Ethylbenzene was placed in a stainless-steel vessel connected to the flow manifold through a fine metering valve. Ethylbenzene was introduced by heating the vessel and the contained liquid to a temperature 5−10 K above the boiling point and adjusting the exit valve to deliver the intended partial pressures, which were confirmed chromatographically. Styrene (Sigma-Aldrich, 99.5+%, stabilized with 4-*tert*-butylcatechol) was dried using freshly calcined (723 K, 12

https://doi.org/10.1021/acscatal.5c04904
ACS Catal. 2025, 15, 19102−19110

h) 4A molecular sieves. Styrene was introduced using a syringe pump (KD Scientific Legato 100) connected to the flow manifold (resistively heated to 373 K and exhibiting no detectable background reactivity) through a rubber septum.

The identity and concentration of species in the reactor effluent were determined by online gas chromatography (Agilent 6890A GC) using flame ionization detection (FID) after separation in a capillary column (Agilent; HP-1) and thermal conductivity detection (TCD) after separation in a Porapak Q column. Products were identified in the chromatographs by comparing their retention times to those of chemical standards and from analysis of representative gas samples by mass spectrometry after similar chromatographic protocols (Agilent 6890A equipped with 5975C MS).

Rates were measured over a range of pressures of hydrocarbons (1−5 kPa) and H_2 (5−30 kPa). They are reported as molar rates of formation of the respective product per mass (gravimetric rates). Dehydrogenation rates r_f were determined by correcting the measured rates r_n for approach to equilibrium, calculated from the mean reactor gas composition and the equilibrium constant (K_{dehyd}) for the dehydrogenation of ethylbenzene according to eq 1.

$$r_f = r_n(1 - \eta)^{-1} \tag{1}$$

The approach to equilibrium values η were computed by the quotient of the measured concentrations of gases in the effluent and the equilibrium constant (K_{dehyd}) for the reaction at the temperature of the reactor where the units of pressure are consistent (e.g., bar):

$$\eta = \frac{[C_8H_8][H_2]}{[C_8H_{10}]} K_{dehyd}^{-1} \tag{2}$$

Similarly, styrene hydrogenation rates were determined from measured hydrogenation rates corrected for the corresponding approach to equilibrium.

Selectivities are reported on a carbon basis as the ratio of converted hydrocarbon molecules that formed the product to those formed from C−C bond scission events.

3. RESULTS AND DISCUSSION

3.1. Ethylbenzene Dehydrogenation and Styrene Hydrogenation Rate Enhancement by Chemical Treatments of *m*-ZrO_2 Surfaces. Table 1 shows gravimetric rates of ethylbenzene dehydrogenation (at 723 K) and styrene hydrogenation (at 523 K) on *m*-ZrO_2 samples treated in He and then with DME (1.5 kPa, 0.9 ks) at 723 K. Ethylbenzene dehydrogenation rates increased 62-fold (from 0.015 to 0.94 mol kg^{-1} h^{-1}) when He-treated m-ZrO_2 catalysts were subsequently treated with DME at 723 K. DME treatments also increased the rates of styrene hydrogenation (50-fold; Table 1). The magnitude of these DME-induced rate enhancements resemble those reported previously for ethane dehydrogenation[17] (74-fold; 773 K, Table 1) and ethene hydrogenation (82-fold). The effects of chemical treatment in uncovering the most competent sites for the C−H and H−H cleavage and formation steps involved in these reactions indicate that the low-coordination Zr−O LAB pairs that mediate C_2−C_4 alkane dehydrogenation and C_2−C_4 alkene hydrogenation are also involved in ethylbenzene dehydrogenation and styrene hydrogenation turnovers. The similar effects of DME treatments on ethylbenzene dehydrogenation (and styrene hydrogenation) and C_2−C_4 alkane dehydrogenation[17] (and alkene hydrogenation) attest, in turn, to the general and useful impacts of such treatments on reactivity and to their role in uncovering uniquely active sites; these are sites that do not survive desorptive removal processes requiring higher temperatures, because of the sintering and annealing processes that accompany such treatments.

Table 1. Rates of Ethane and Ethylbenzene Dehydrogenation and Reverse Ethylene and Styrene Hydrogenation on *m*-ZrO_2 Treated in He or DME at 723 K at Conditions Described in the Footnotes

	Reactant	He-treated *m*-ZrO_2	DME-treated *m*-ZrO_2	Enhancement Factor[a]
Dehydrogenation rates, mol·kg^{-1}·h^{-1}	C_2H_6[b]	0.19	14	74
	C_8H_{10}[c]	0.015	0.94	62
Hydrogenation rates, mol·kg^{-1}·h^{-1}	C_2H_4[d]	2.8	230	82
	C_8H_8[e]	0.3	15	50

[a]Enhancement factors are defined as rates on samples treated with He (100 kPa, 1.8 ks) and then DME (1.5 kPa, 0.9 ks) at 723 K divided by those on samples treated in He (100 kPa, 1.8 ks) at 723 K. [b]15 kPa C_2H_6, 5.1 kPa H_2, 773 K. [c]1.8 kPa C_8H_{10}, 12 kPa H_2, 723 K. [d]9.2 kPa C_2H_4, 5.6 kPa H_2, 723 K. [e]1.9 kPa C_8H_8, 12 kPa H_2, 573 K.

The kinetic trends and the unique reactivity and selectivity of the Zr−O LAB pairs uncovered by chemical treatments at *m*-ZrO_2 surfaces were recently shown for dehydrogenation of small alkanes,[17] which rendered *m*-ZrO_2 uniquely competent as catalysts for these reactions. The results described next indicate that the unique reactivity and selectivity of Zr−O LAB pairs can be extended to the dehydrogenation and hydrogenation reactions of alkyl side chains in arenes, leading to rates and selectivities that exceed those of the most competent styrene production catalysts.

3.2. Kinetic Effects of Ethylbenzene, Styrene, and H_2 Pressures on Dehydrogenation and Hydrogenation Rates on DME-Treated *m*-ZrO_2 Surfaces. Ethylbenzene dehydrogenation rates on DME-treated *m*-ZrO_2 (corrected for approach to equilibrium where required, eq 1) are strictly proportional to ethylbenzene pressure (1−6 kPa) and independent of H_2 pressure (5−25 kPa) (723 K; Figure 1). These trends are consistent with the stoichiometry of the overall dehydrogenation reaction and with the law of mass action kinetics and lead to forward rates (r_{dehyd}) given by

$$r_{dehyd} = k_{dehyd} \cdot (C_8H_{10}) \tag{3}$$

where k_{dehyd} is the dehydrogenation rate parameter and (C_8H_{10}) is the ethylbenzene pressure. Rate equations that reflect the respective reaction stoichiometries also describe C_2−C_4 alkane dehydrogenation rates on *m*-ZrO_2.[17] These trends indicate that kinetically relevant C−H activation steps occur on Zr−O pairs that remain essentially bare during dehydrogenation turnovers. The molecular stoichiometry of the kinetically relevant transition state (TS) must correspond, in such cases, to that of an ethylbenzene molecule in order to account for the functional form of eq 3.

Lewis acid−base site pairs at *m*-ZrO_2 surfaces also catalyze styrene hydrogenation to ethylbenzene (the reverse reaction), and DME treatments increase hydrogenation rates (over He treatments) to similar extents to that for ethylbenzene dehydrogenation (Table 1). Hydrogenation rates (r_{hyd}; corrected for approach to equilibrium, eq 1) are proportional

https://doi.org/10.1021/acscatal.5c04904
ACS Catal. 2025, 15, 19102−19110

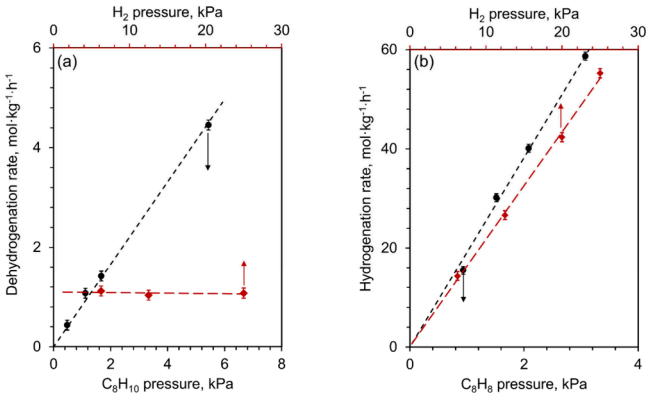

Figure 1. a) C_8H_{10} (ethylbenzene) dehydrogenation rates (per mass) on DME-treated (at 723 K, 1.5 kPa DME, 0.9 ks) *m*-ZrO_2 as a function of C_8H_{10} pressure (bottom axis, black; 13.5 kPa H_2) and H_2 pressure (top axis, red; 1.3 kPa C_8H_{10}) at 723 K. b) C_8H_8 (styrene) hydrogenation rates on DME-treated (at 723 K, 1.5 kPa DME, 0.9 ks) *m*-ZrO_2 as a function of C_8H_8 pressure (bottom axis, black, 13.5 kPa H_2) and H_2 pressure (top axis, red, 1 kPa C_8H_8) at 623 K. Dashed lines are to guide the eye. Error bars represent 95% confidence intervals calculated from 5 replicates.

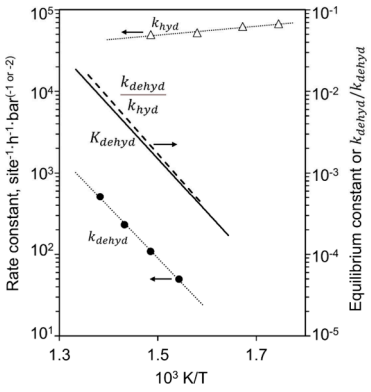

Figure 2. First-order rate constants for C_8H_{10} dehydrogenation (k_{dehyd}, closed circles; eq 3) and second-order rate constants for C_8H_8 hydrogenation (k_{hyd}, open triangles; eq 4) on DME-treated (723 K) *m*-ZrO_2 plotted in Arrhenius-type form with comparisons to the equilibrium constant (K_{dehyd}, solid line) and to the ratio of k_{dehyd}/k_{hyd} (dashed line). Dotted lines from exponential regression.

to both styrene (1−3 kPa) and H_2 (7−25 kPa) pressures on DME-treated *m*-ZrO_2 (Figure 1; 623 K) and described by

$$r_{hyd} = k_{hyd}\cdot(C_8H_8)\cdot(H_2) \tag{4}$$

where k_{hyd} is the rate constant for hydrogenation and (C_8H_8) and (H_2) are the respective reactant pressures. As for the dehydrogenation direction, these kinetic trends reflect the stoichiometry of the overall reaction and the law of mass action, indicating that the kinetically relevant step for styrene hydrogenation also occurs on LAB site pairs that remain essentially devoid of bound intermediates or spectators derived from reactants or products. These kinetic trends also show that the stoichiometry of the kinetically relevant TS corresponds to one styrene and one H_2 molecule.

3.3. Mechanistic and Thermodynamic Links between Dehydrogenation and Hydrogenation Rates. The same LAB pairs catalyze ethylbenzene dehydrogenation and its reverse reaction (styrene hydrogenation), as evident from DME treatments, which lead to similar rate enhancements for dehydrogenation and hydrogenation reactions. Kinetic trends for each reaction reflect their respective reaction stoichiometries (eqs 3 and 4), and both reactions occur on essentially bare Zr−O pairs through kinetically relevant transition states with the same atomic stoichiometry (C_8H_{10}). Site-normalized rate constants for each reaction were determined by measuring the number of active sites on *m*-ZrO_2 using H_2O titration protocols during propane dehydrogenation, enabling estimates of the intrinsic reactivity of LAB sites for these reactions.[17]

Figure 2 shows the effects of the temperature on ethylbenzene dehydrogenation and styrene hydrogenation rate constants (per site) on DME-treated *m*-ZrO_2. Rate parameters increased exponentially with temperature for dehydrogenation (activation energy: 115 ± 11 kJ·mol^{-1}), but decreased exponentially for hydrogenation (−12 ± 3 kJ mol^{-1}), the latter with negative barriers that reflect a kinetically relevant styrene hydrogenation TS lower in enthalpy than the bare site and gaseous H_2 and styrene molecules from which it forms.

Both forward and reverse reactions occur on bare Zr−O pairs, and rate constants for the kinetically relevant step in each direction are given by

$$k_{dehyd} = \frac{k_bT}{h}e^{-(\Delta G^{\ddagger,0}_{dehyd})/RT} = \frac{k_bT}{h}e^{-(\Delta G^0_{TS(dehyd)}-\Delta G^0_{EtBz}-\Delta G^0_{Zr-O})/RT} \tag{5}$$

$$k_{hyd} = \frac{k_bT}{h}e^{-(\Delta G^{\ddagger,0}_{hyd})/RT} = \frac{k_bT}{h}e^{-(\Delta G^0_{TS(hyd)}-\Delta G^0_{STY}-\Delta G^0_{H_2}-\Delta G^0_{Zr-O})/RT} \tag{6}$$

where k_b is the Boltzmann constant, h is Planck's constant, $\Delta G^{\ddagger,0}_{dehyd}$ reflects the free energy of formation of TS mediating dehydrogenation ($\Delta G^0_{TS(dehyd)}$) from a gaseous ethylbenzene molecule (ΔG^0_{EtBz}) and a bare Zr−O site pair ($\Delta G^0_{Zr\text{-}O}$), $\Delta G^{\ddagger,0}_{hyd}$ is the free energy of formation of TS mediating the hydrogenation pathway ($\Delta G^0_{TS(hyd)}$) from the gaseous styrene (ΔG^0_{STY}), H_2 ($\Delta G^0_{H_2}$), and a bare Zr−O site pair. The ratio of these forward and reverse rate constants is

$$\frac{k_{dehyd}}{k_{hyd}} = e^{-(\Delta G^{\ddagger,0}_{dehyd}-\Delta G^{\ddagger,0}_{hyd})/RT} = e^{-(\Delta G^0_{TS(dehyd)}-\Delta G^0_{TS(hyd)})/RT}\cdot e^{-\Delta G^0_{STY}+\Delta G^0_{H_2}-\Delta G^0_{EtBz}/RT} = e^{-(\Delta G^0_{TS(dehyd)}-\Delta G^0_{TS(hyd)})/RT}\cdot K_{dehyd} \tag{7}$$

This ratio of rate constants depends on the difference in free energies of the transition states in the two directions and the equilibrium constant for the overall reaction (K_{dehyd}) at each temperature. The measured ratio of forward and reverse rate constants (k_{dehyd}/k_{hyd}) is nearly identical to K_{dehyd} at each temperature (Figure 2), showing that the hydrogenation and dehydrogenation TS are identical in free energy, in line with their identical atomic stoichiometry. Dissecting the free energies in eq 7 into enthalpy and entropy components gives

$$\frac{k_{dehyd}}{k_{hyd}} = e^{-(\Delta H^0_{rxn})/RT}\cdot e^{(\Delta S^0_{rxn})/R} \tag{8}$$

https://doi.org/10.1021/acscatal.5c04904
ACS Catal. 2025, 15, 19102−19110

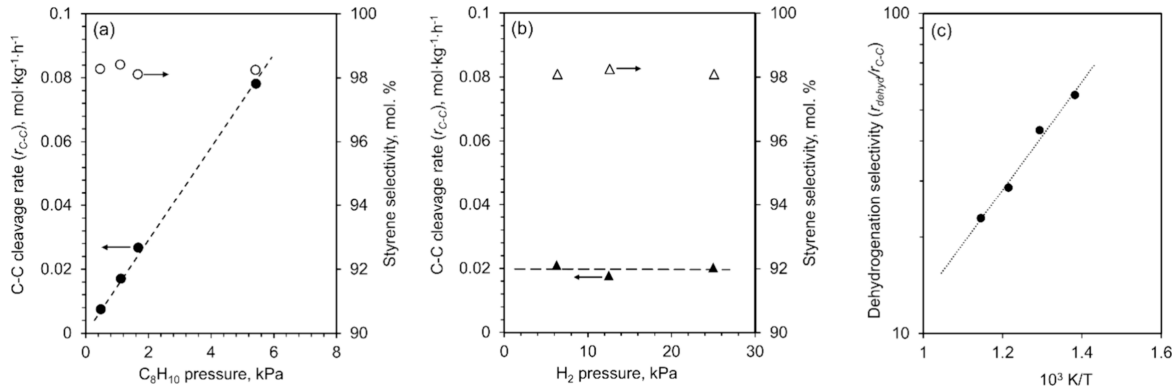

Figure 3. C−C cleavage rates (per mass, closed symbols, left) and styrene molar selectivities (open symbols, right) on DME-treated (at 723 K, 1.5 kPa DME, 0.9 ks) *m*-ZrO_2 as a function of (a) C_8H_{10} pressure (13.5 kPa H_2) and (b) H_2 pressure (1.3 kPa C_8H_{10}) at 723 K. Dashed lines are to guide the eye. c) Dehydrogenation selectivities r_{dehyd}/r_{C-C} on DME-treated (at 723 K, 1.5 kPa DME, 0.9 ks) *m*-ZrO_2 plotted versus reciprocal temperature. Dotted lines from exponential regression.

where ΔH^0_{rxn} and ΔS^0_{rxn} are the changes in enthalpy and entropy for the overall reaction. The difference between measured dehydrogenation and hydrogenation activation barriers (127 ± 13 kJ mol^{-1}; from $\frac{k_{dehyd}}{k_{hyd}}$; Figure 2) is similar to the dehydrogenation reaction enthalpy (ΔH_{rxn}: +125 kJ mol^{-1}),[25] indicative of a kinetically relevant TS that is similar in enthalpy for the two directions. This is also the case for activation entropies (ΔS_{rxn} +143 ± 17 J mol^{-1} K^{-1}; Figure 2; +135 J mol^{-1} K^{-1}, for the reaction entropy[25]).

The $\frac{k_{dehyd}}{k_{hyd}}$ ratio in eqs 7 and 8 is analogous to one that can be derived from De Donder relations:[26]

$$\frac{\vec{r}_i}{\overleftarrow{r}_i} = e^{-(A_i)/RT} = K_i \prod_j a_j^{-\nu_j} \tag{9}$$

that relate forward ($\vec{r}_i$) and reverse ($\vec{r}_i$) rates of an elementary step to the chemical affinity (A_i), which can be expressed though the equilibrium constant (K_i) and activities (a_j) and molecularities (ν_j) of species involved. De Donder relations generally apply to individual elementary steps but not for their sequences. Extending to sequences requires that forward and reverse reactions (i) involve the same kinetically relevant step at the respective (different) conditions used to measure their rates and (ii) occur on surfaces predominantly covered by the same intermediate at the conditions used in the two directions (a condition unlikely to be met except for essentially bare sites).[27−31] These two conditions are met for ethylbenzene dehydrogenation and styrene hydrogenation, as shown by their respective kinetic trends (Figure 1) and consistent with the thermodynamic relations that rigorously link the rate constants for the forward and reverse reactions (Figure 2). These links between thermodynamic and kinetic parameters allow accurate estimates of rates in one direction from those measured in the other direction and tabulated thermodynamic data for gaseous species.

3.4. Selectivity of LAB Pairs Ethylbenzene Dehydrogenation and Styrene Hydrogenation. Ethylbenzene reactions at 723−873 K on DME-treated catalysts form predominantly styrene and H_2 and trace exocyclic C−C cleavage products without detectable ring opening or hydrogenation. C−C cleavage rates (r_{C-C}) were proportional to ethylbenzene pressure (Figure 3a) and unaffected by H_2 (Figures 3b and S1) or conversion (as rates decreased with time; Figure S2), consistent with C−C cleavage via primary reactions of ethylbenzene. Dehydrogenation selectivities (dehydrogenation to C−C cleavage rate ratios; r_{dehyd}/r_{C-C}) are unaffected by the reactant or product pressures. Higher temperatures favor C−C cleavage over dehydrogenation, which is a reflection of the higher activation energy for C−C cleavage (Figures 3c and S3; 146 ± 18 kJ·mol^{-1}) than dehydrogenation (115 ± 11 kJ·mol^{-1}; Figure 2). The r_{dehyd}/r_{C-C} values remain larger than 25 even at 873 K, and styrene selectivities (>95%) are similar to those on the best reported catalysts (e.g., K-FeO_x; 95−97%,[1,3,4] 873 K, Table S1).

3.5. Benchmarking Ethylbenzene Dehydrogenation Rates on Chemically Treated *m*-ZrO_2 against State-of-the-Art Catalysts. Ethylbenzene dehydrogenation catalysts typically consist of Fe-based solids with K, Mg, Mo, and Ce promoters.[1,3,4] Other catalytic systems such as Ca, Sr, and Ba zirconates,[12] zeolites doped with Fe,[14] activated carbon materials,[11] and MoO_3 domains on ZrO_2[13] have also been reported. Ethylbenzene dehydrogenation rates (gravimetric; per mass) on DME-treated *m*-ZrO_2 are compared with those of the most competent catalysts reported previously in Table S1. Most previous reports do not describe pressure or temperature effects on rates; consequently, kinetic trends reported here on DME-treated *m*-ZrO_2 are used to estimate the rates and selectivities on this catalyst under the conditions used to measure rates in each previous study. Gravimetric dehydrogenation rates on DME-treated *m*-ZrO_2 are 10−100 times larger than those on most reported catalysts (Figure 4). These performance benchmarks attest to the competence and practical relevance of earth-abundant *m*-ZrO_2 catalysts that are chemically treated to uncover their most competent C−H activation (and formation) sites.

3.6. Chemical Dehydroxylation of *m*-ZrO_2 Surfaces by Reactants during Ethylbenzene Dehydrogenation Catalysis. Ethylbenzene dehydrogenation rate enhancements observed after DME treatments (723 K, 1.5 kPa DME, 0.9 ks) of *m*-ZrO_2 (Table 1) decrease with the reaction time at rates that depend on the concentration of trace impurities in reactants. Initial rates are similar to ethylbenzene reactants (Sigma-Aldrich, 99.5+%) used without further treatments (denoted as "nonpurified", 3.9 mol·kg^{-1}·h^{-1}), when they were treated by contact with 4A sieves (treated at 723 K, 5 h, air) before use (denoted as "purified", 4.2 mol·kg^{-1}·h^{-1}) and when they were freshly distilled on HFAU molecular sieves

https://doi.org/10.1021/acscatal.5c04904
ACS Catal. 2025, 15, 19102−19110

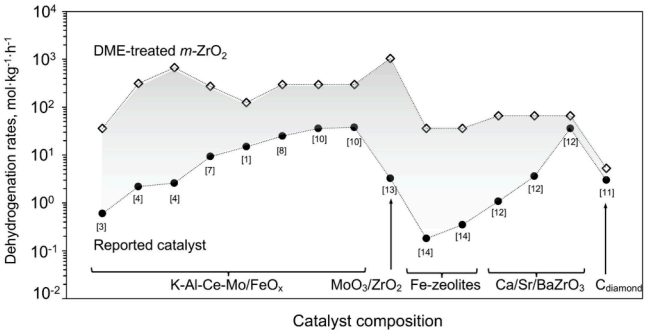

Figure 4. Gravimetric ethylbenzene dehydrogenation rates on previously reported catalysts (alkali-promoted Fe-based catalysts, Fe-containing zeolites, Ca, Sr, and Ba zirconates, activated carbon materials, and dispersed MoO_3 domains) compared to expected dehydrogenation rates on DME-treated m-ZrO_2 using the rate relations shown in eq 3 and Figures 2 and 3. References to the previous literature indicated for each sample and cited in the reference list at the end of this article.

and afterward twice treated by contact with freshly calcined 4A sieves (denoted as "rigorously purified", 4.0 mol·kg^{-1}·h^{-1}). Notably, rates decreased significantly more slowly as reactant streams are purified more thoroughly (Figure 5a). The observed "deactivation" merely reflects the titration of the sites uncovered by DME treatments with H_2O (or its O_2 precursors), as also shown by the full recovery of initial rates by subsequent DME treatments (at 723 K, Figure S4). Direct quantification of LAB sites on m-ZrO_2 was achieved by *in situ* titration with H_2O, which provides a reliable measure of LAB density and correlates with catalytic activity trends and the amounts of H_2O released from m-ZrO_2 during temperature-programmed desorption.[17,18] Areal densities of Zr−O pairs measured from H_2O stoichiometric titrations (0.56 nm^{-2}) on these m-ZrO_2 samples[17,18] were used to estimate H_2O levels in reactant streams (43, 10, and 4 ppm for nonpurified, purified, and rigorously purified ethylbenzene reactants, respectively, details in SI, Section 1.6). Dehydrogenation rates ultimately reached asymptotic values, suggesting that a fraction of the sites responsible for rates (and titrated by strongly bound H_2O) persist indefinitely under the reaction conditions. These asymptotic rates strongly depend on ethylbenzene purifications, suggesting that H_2O levels affect asymptotic rates and that the fraction of sites that persist in the presence of reactants remain uncovered.

Asymptotic rates with purified reactants are about 3-fold higher than the initial rates on m-ZrO_2 treated in He at 773 K, indicating that the number of persistent sites exceeds that present upon initial contact with reactants after thermal treatments. Rates increased with time with purified ethylbenzene reactants and reached the same asymptotic rates observed on m-ZrO_2 treated with DME (Figure 5b). Similarly, an increase in the rates was observed with rigorously purified reactants, where asymptotic rates of 70% of the initial rates on DME-treated m-ZrO_2 catalysts are achieved (Figure 5c). Notably, these asymptotic rates remained stable for >50 ks (Figure S5).

Thus, the initial rates depend on the number of LAB sites uncovered by a given treatment (He vs DME), but the temporal evolution of rates and their asymptotic values reflect the concentration of titrants in reactant streams. The observed increase in rate on He-treated m-ZrO_2 must reflect the ability of ethylbenzene reactants (or styrene products) to offset, in part, the titration of sites by prevalent H_2O levels through chemical scavenging processes similar to those mediated by DME during pretreatments. Ethylbenzene reactions with surface hydroxyls, as in the case of DME treatments, remove strongly bound H_2O molecules from low-coordination Zr−O Lewis acid−base pairs. These hydroxylated sites are the most competent sites for C−H cleavage and formation, but they remain covered by dissociated water and are unable to bind ethylbenzene as the reactant in dehydrogenation turnovers. Low-coordination Zr−O LAB pairs stabilize both H_2O adsorption and the kinetically relevant transition states most effectively. The removal of bound H_2O from such sites, whether by DME or by hydrocarbon treatments, uncovers them and restores the activity of pre-existing low-coordination Zr−O pairs without requiring thermal treatments at higher temperatures, which restructure or destroy them. Importantly, both site titration with H_2O and regeneration with DME are performed in the same reactor at 723 K, minimizing the possibility of structural changes other than those induced by the intended chemical reactions.[17,18] The areal densities of persistent LAB pairs at steady state would then reflect the balance between the rates of H_2O binding onto sites and their removal by reaction with ethylbenzene (or styrene). Asymptotic rates that did not depend on styrene partial pressures (varied through changes in residence time; Figure

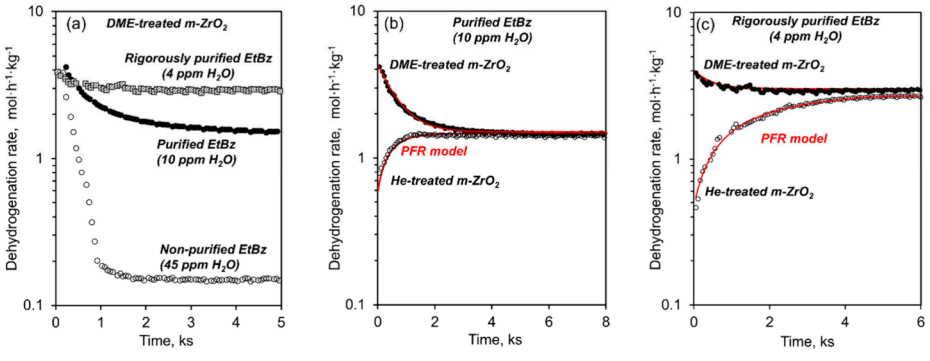

Figure 5. a) Ethylbenzene dehydrogenation rates (773 K, 1.2 kPa EtBz, 12 kPa H_2) on DME-treated (723 K, 1.5 kPa DME, 0.9 ks) m-ZrO_2 using nonpurified (open circles), purified (closed circles), and rigorously purified (dashed squares) ethylbenzene reactants. b,c) Ethylbenzene dehydrogenation rates under the same conditions on DME-treated (closed circles) or He-treated (open circles) m-ZrO_2 using purified (b) and rigorously purified (c) ethylbenzene reactants. Rates predicted according to the PFR model are shown in red solid lines.

https://doi.org/10.1021/acscatal.5c04904
ACS Catal. 2025, 15, 19102−19110

Scheme 1. Schematic Depiction of the Coupled Diffusion−Convection−Reaction System for Ethylbenzene (EtBZ) Dehydrogenation on the Zr−O LAB Pair (*): (I) EtBZ Dehydrogenation to Styrene (STY) and H_2 on *, (II) * Titration with H_2O Forming Titrated LAB Pair Site (H_2O*), and (III) H_2O* Cleaning with EtBz Forming X Where X Binds More Weakly than H_2O

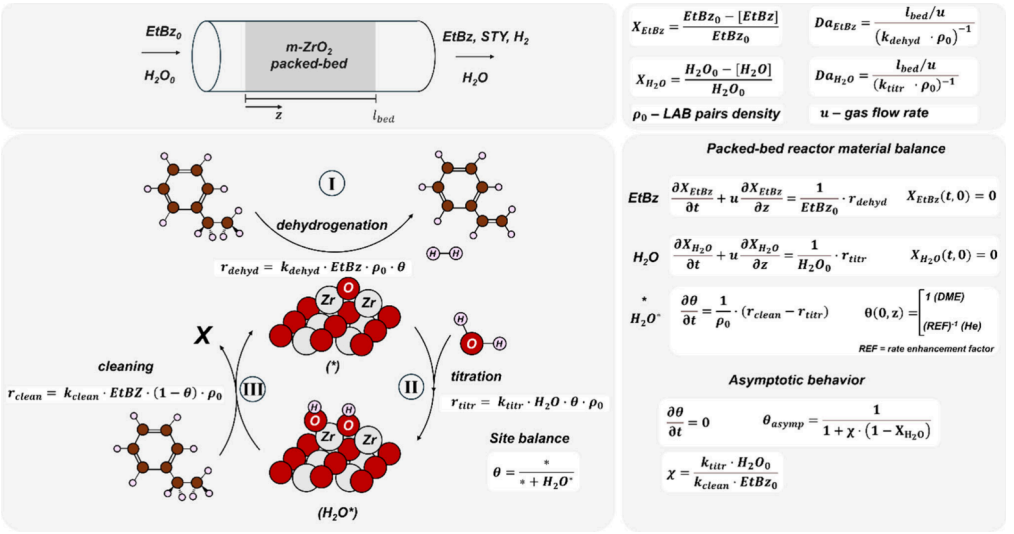

S5) indicate that ethylbenzene is the predominant scavenger of bound H_2O species, at least at the low ethylbenzene conversions tested (0.5−2%). The products of ethylbenzene reaction with strongly bound H_2O, which uncover LAB pairs, are well below detection limits (present at ∼10 ppm; see Section S1.3; Supporting Information) during ethylbenzene dehydrogenation catalysis, because of their very slow formation over the extended times required for their effects on dehydrogenation rates and the very small areal density of these H_2O-binding Zr−O sites. These reactions are expected to involve the hydroxylation of the benzene ring analogously to propene reactions with surface hydroxyls on oxides that have been reported to produce propanol.[32−34]

Scheme 1 depicts these inferences as specific chemical reactions and their respective rate equations:

(I) First-order ethylbenzene (EtBz) dehydrogenation to styrene (STY) and H_2 at uncovered LAB sites (*) with a rate constant k_{dehyd} (eq 3),

(II) H_2O binding at * with rate proportional to H_2O concentration and to * fraction and with a rate constant k_{titr} forming titrated LAB pair site H_2O*,

(III) H_2O* cleaning with EtBz with a rate constant k_{clean} regenerating * and forming X (e.g., via hydrolysis of the side chain or aromatic ring), where X binds much more weakly than H_2O on *.

Reaction−convection mole balances for EtBz and H_2O and for temporal changes in the fractional coverages of titrant-free sites (θ) are (derivation details; Section 1.7; SI) as follows:

$$\frac{\partial X_{\mathrm{EtBz}}}{\partial \xi} = \mathrm{Da}_{\mathrm{EtBz}} \cdot \theta \tag{10}$$

$$\frac{\partial X_{\mathrm{H_2O}}}{\partial \xi} = \mathrm{Da}_{H_2O} \cdot \theta \cdot (1 - X_{H_2O}) \tag{11}$$

$$\tau_{clean} \frac{\partial \theta}{\partial t} = (1 - \theta) - \chi \cdot (1 - X_{H_2O}) \cdot \theta \tag{12}$$

where X_{EtBz} and $X_{\mathrm{H_2O}}$ are EtBz and H_2O fractional conversions at each axial position and time; $\mathrm{Da}_{\mathrm{EtBz}}$ and $\mathrm{Da}_{\mathrm{H_2O}}$ are Damköhler dimensionless parameters that account for the ratio of bed residence time to characteristic times for EtBz dehydrogenation or H_2O binding reactions, respectively; ξ is dimentionless bed length coordinate, τ_{clean} is the characteristic time of cleaning reaction; and χ reflects the ratio of titration to cleaning rates at inlet concentrations of H_2O and EtBz (Scheme 1). Inlet stream compositions determine boundary conditions for X_{EtBz} and $X_{\mathrm{H_2O}}$, and catalyst treatments applied before reactions define initial conditions for θ (all sites are titrant-free for DME treatments and sites are partially covered with H_2O for He treatments, Scheme 1).

The short bed residence times used in these experiments led to a ratio of convection characteristic time to characteristic times of ethylbenzene chemical reaction ($\mathrm{Da}_{\mathrm{EtBz}} \ll 1$), leading to spatial gradients evolving over time scales much longer than bed residence times (SI, Section 1.7) and, consequently, to nearly constant axial EtBz concentrations throughout the bed at all times. Dehydrogenation rates vary with time, because of the temporal evolution of θ. This model can be used to regress $\theta(t)$ transients (from observed dehydrogenation rate changes with time) during reactions on DME-treated m-ZrO_2 (Section 1.7, SI).

Equations 10−12 and the parameters obtained from these regressions accurately described the temporal changes in rates for samples treated with DME or He (Figure 5b), and fitting yields higher initial rates of H_2O binding than for H_2O* scavenging reactions ($\chi \gg 1$) on * prevailing surfaces. When H_2O molecules are introduced with the inlet streams, they bind rapidly to *, which prevails on DME-treated surfaces, leading to a decrease in θ (and, consequently, to lower dehydrogenation rates). Over time, coverage of H_2O* increases, leading to lower titration rates and higher scavenging (cleaning) rates. Ultimately, titration and scavenging rates equilibrate, and θ reaches asymptotic values (θ_{asymp}, eq 13):

https://doi.org/10.1021/acscatal.5c04904
ACS Catal. 2025, 15, 19102−19110

$$\theta_{asymp} = \frac{1}{1 + \chi \cdot (1 - X_{H_2O})} \quad (13)$$

These θ_{asymp} values define the asymptotic dehydrogenation rates, which are governed by the balance between titration and cleaning processes (χ) and depend strongly on inlet H_2O concentrations and its conversion. A 4-fold decrease in H_2O concentration (from 43 to 10 ppm) led to 7-fold higher asymptotic rates (Figure 5 b), and further decrease of H_2O content to 4 ppm by rigorous purification lead to an additional 2-fold increase in asymptotic rates, reaching 70% of initial rates on the DME-treated m-ZrO_2 catalyst. The model indicates that a further decrease in H_2O levels to 1 ppm would lead to asymptotic rates of 0.95 of the initial rates on the DME-treated catalyst (Figure 6), essentially eliminating deactivation.

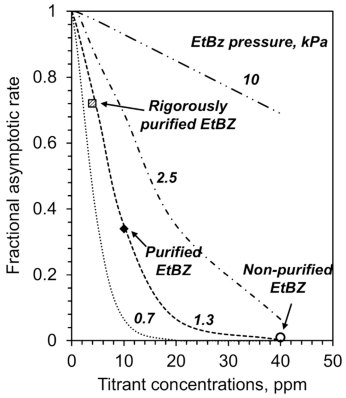

Figure 6. Predicted fractional asymptotic ethylbenzene dehydrogenation rates on *m*-ZrO_2 (12.5 kPa H_2, 773 K) for different inlet titrant concentrations and EtBz pressures. Markers correspond to experimental measurements; numbers next to curves correspond to different EtBz partial pressures.

Increasing the ethylbenzene concentration at constant titrant levels similarly enhances scavenging rates, further raising asymptotic rates (Figure 6). These asymptotic rates can be reached without DME treatment (Figure S7), as evident from He-treated *m*-ZrO_2 catalyst activation when purified ethylbenzene is used (Figure 5b), indicating that reactant-induced uncovering of LAB sites is possible if inlet H_2O (and O_2) levels are sufficiently low.

4. CONCLUSIONS

Chemically-treated monoclinic ZrO_2 (*m*-ZrO_2) surfaces expose low-coordination Lewis acid−base (LAB) pairs that catalyze nonoxidative dehydrogenation of ethylbenzene to styrene and its reverse hydrogenation with exceptional activity and selectivity. These site pairs remain essentially unoccupied during catalytic turnovers, leading to rate laws that follow the law of mass action in both directions. Forward and reverse reaction sequences proceed through the same kinetically relevant transition state, resulting in thermodynamically coupled rate constants and enabling an accurate prediction of the rate in one direction from that measured in the other.

Chemical dehydroxylation using dimethyl ether (DME) removes strongly bound H_2O titrants without harsh thermal treatments, increasing reaction rates by more than 60-fold and preserving the structural integrity of low-coordination LAB pairs. Ethylbenzene itself can also scavenge H_2O titrants, achieving asymptotic rates governed by the balance of titration and scavenging kinetics and allowing stable operation without DME treatment.

Gravimetric dehydrogenation rates on DME-treated *m*-ZrO_2 surpass those of benchmark Fe-based catalysts by up to 20-fold, while maintaining styrene selectivities above 95%. These findings underscore the practical relevance of earth-abundant oxides and the critical role of surface chemistry control in enabling efficient steam-free styrene production.

■ ASSOCIATED CONTENT

Supporting Information

The Supporting Information is available free of charge at https://pubs.acs.org/doi/10.1021/acscatal.5c04904.

Rates of terminal and nonterminal C−C cleavage and corresponding styrene selectivities; selectivity trends with conversion; Arrhenius plots of C−C cleavage rate constants; ethylbenzene dehydrogenation deactivation and reactivation behavior at different reactant purities; long-term stability of DME-treated catalysts and effects of space velocity; benchmarking data for reported ethylbenzene dehydrogenation catalysts; derivation of De Donder relations; development of plug-flow reactor kinetic model (PDF)

■ AUTHOR INFORMATION

Corresponding Author

Enrique Iglesia − *Department of Chemical and Biomolecular Engineering, University of California at Berkeley, Berkeley, California 94720, United States; Davidson School of Chemical Engineering, Purdue University, West Lafayette, Indiana 47907, United States;* orcid.org/0000-0003-4109-1001; Email: iglesia@berkeley.edu

Authors

Mikalai A. Artsiusheuski − *Department of Chemical and Biomolecular Engineering, University of California at Berkeley, Berkeley, California 94720, United States;* orcid.org/0000-0003-4931-9568

Nicholas R. Jaegers − *Department of Chemical and Biomolecular Engineering, University of California at Berkeley, Berkeley, California 94720, United States;* orcid.org/0000-0002-9930-7672

Carlos Lizandara-Pueyo − *BASF SE, 67056 Ludwigshafen am Rhein, Germany;* orcid.org/0000-0003-1146-775X

Complete contact information is available at: https://pubs.acs.org/10.1021/acscatal.5c04904

Notes

The authors declare the following competing financial interest(s): The authors have filed provisional patents applications for the preparation of metal oxide catalysts with LAB pairs and their applications in dehydrogenation reactions.

■ ACKNOWLEDGMENTS

We acknowledge BASF for financial support and technical guidance through the California Research Alliance. We acknowledge Dr. Andrew Hwang for discussions on plug flow reactor modeling.

REFERENCES

(1) Lee, E. H. Iron Oxide Catalysts for Dehydrogenation of Ethylbenzene in the Presence of Steam. *Catal. Rev.* **1974**, *8* (1), 285−305.

(2) Cavani, F.; Trifirò, F. Alternative Processes for the Production of Styrene. *Appl. Catal. A, Gen.* **1995**, *133* (2), 219−239.

(3) Oliveira, A. C.; Fierro, J. L. G.; Valentini, A.; Nobre, P. S. S.; Rangel, M. do C. Non-Toxic Fe-Based Catalysts for Styrene Synthesis: The Effect of Salt Precursors and Aluminum Promoter on the Catalytic Properties. *Catal. Today* **2003**, *85* (1), 49−57.

(4) Baghalha, M.; Ebrahimpour, O. Structural Changes and Surface Activities of Ethylbenzene Dehydrogenation Catalysts during Deactivation. *Appl. Catal. A Gen.* **2007**, *326* (2), 143−151.

(5) Luyben, W. L. Design and Control of the Styrene Process. *Ind. Eng. Chem. Res.* **2011**, *50* (3), 1231−1246.

(6) Dimian, A. C.; Bildea, C. S. Energy Efficient Styrene Process: Design and Plantwide Control. *Ind. Eng. Chem. Res.* **2019**, *58* (12), 4890−4905.

(7) Zhang, Z.; Zeng, T.; Wei, C.; Song, L.; Miao, C. Ce-Promoted Fe-K-Mg Catalyst and Its Application in Dehydrogenation of Ethylbenzene. *Mol. Catal.* **2023**, *540*, 113058.

(8) Li, Y.; Cui, Y.; Zhang, X.; Lu, Y.; Fang, W.; Yang, Y. Optimum Ratio of K2O to CeO2 in a Wet-Chemical Method Prepared Catalysts for Ethylbenzene Dehydrogenation. *Catal. Commun.* **2016**, *73*, 12−15.

(9) Abe, K.; Kano, Y.; Ohshima, M. A.; Kurokawa, H.; Miura, H. Effect of Adding Mo to Fe-Ce-K Mixed Oxide Catalyst on Ethylbenzene Dehydrogenation. *J. Japan Pet. Inst.* **2011**, *54* (5), 338−343.

(10) Zha, K.; Zeng, T.; Zhu, M.; Wei, C.; Song, L.; Miao, C. Insights into Promotional Effects for Ethylbenzene Dehydrogenation to Styrene with Steam over Fe-K, Fe-K-Ce and Fe-K-Ce-Mo Mixed Oxide Catalysts. *Appl. Catal. A Gen.* **2023**, *666*, 119372.

(11) Zhang, J.; Su, D. S.; Blume, R.; Schlögl, R.; Wang, R.; Yang, X.; Gajović, A. Surface Chemistry and Catalytic Reactivity of a Nanodiamond in the Steam-Free Dehydrogenation of Ethylbenzene. *Angew. Chemie - Int. Ed.* **2010**, *49* (46), 8640−8644.

(12) Watanabe, R.; Saito, Y.; Fukuhara, C. Dehydrogenation of Ethylbenzene over Zirconium-Based Perovskite-Type Catalysts of AZrO3 (A: Ca, Sr, Ba). *Appl. Catal. A Gen.* **2014**, *482*, 344−351.

(13) Sancheti, S. V.; Yadav, G. D. Highly Selective Production of Styrene by Non-Oxidative Dehydrogenation of Ethylbenzene over Molybdenum-Zirconium Mixed Oxide Catalyst in Fixed Bed Reactor: Activity, Stability and Kinetics. *Catal. Commun.* **2021**, *154*, 106307.

(14) Bispo, J. R. C.; Oliveira, A. C.; Corrêa, M. L. S.; Fierro, J. L. G.; Marchetti, S. G.; Rangel, M. C. Characterization of FeMCM-41 and FeZSM-5 Catalysts to Styrene Production. *Stud. Surf. Sci. Catal.* **2002**, *142*, 517−524.

(15) Otroshchenko, T.; Sokolov, S.; Stoyanova, M.; Kondratenko, V. A.; Rodemerck, U.; Linke, D.; Kondratenko, E. V. ZrO2-Based Alternatives to Conventional Propane Dehydrogenation Catalysts: Active Sites, Design, and Performance. *Angew. Chemie - Int. Ed.* **2015**, *54* (52), 15880−15883.

(16) Kondratenko, E. V.; et al. ZrO2-Based Unconventional Catalysts for Non-Oxidative Propane Dehydrogenation: Factors Determining Catalytic Activity. *J. Catal.* **2017**, *348*, 282−290.

(17) Jaegers, N. R.; Danghyan, V.; Shangguan, J.; Lizandara-Pueyo, C.; Deshlahra, P.; Iglesia, E. Heterolytic C-H Activation Routes in Catalytic Dehydrogenation of Light Alkanes on Lewis Acid-Base Pairs at ZrO2 Surfaces. *J. Am. Chem. Soc.* **2024**, *146*, 25710−25726.

(18) Jaegers, N. R.; Artsiusheuski, M.; Danghyan, V.; Shangguan, J.; Lizandara-Pueyo, C.; Iglesia, E. Hydrogenation of Alkenes, Cycloalkenes, and Arene Side Chains at Lewis Acid-Base Pairs: Kinetics, Elementary Steps, and Thermodynamic Implications for Reverse Reactions. *ACS Catal.* **2025**, *15*, 12610−12626.

(19) Sun, J.; Baylon, R. A. L.; Liu, C.; Mei, D.; Martin, K. J.; Venkitasubramanian, P.; Wang, Y. Key Roles of Lewis Acid-Base Pairs on ZnxZryOz in Direct Ethanol/Acetone to Isobutene Conversion. *J. Am. Chem. Soc.* **2016**, *138* (2), 507−517.

(20) Komanoya, T.; Nakajima, K.; Kitano, M.; Hara, M. Synergistic Catalysis by Lewis Acid and Base Sites on ZrO2 for Meerwein-Ponndorf-Verley Reduction. *J. Phys. Chem. C* **2015**, *119* (47), 26540−26546.

(21) Radha, A. V.; Bomati-Miguel, O.; Ushakov, S. V.; Navrotsky, A.; Tartaj, P. Surface Enthalpy, Enthalpy of Water Adsorption, and Phase Stability in Nanocrystalline Monoclinic Zirconia. *J. Am. Ceram. Soc.* **2009**, *92* (1), 133−140.

(22) Lackner, P.; Hulva, J.; Köck, E. M.; Mayr-Schmölzer, W.; Choi, J. I. J.; Penner, S.; Diebold, U.; Mittendorfer, F.; Redinger, J.; Klötzer, B.; Parkinson, G. S.; Schmid, M. Water Adsorption at Zirconia: From the ZrO2(111)/Pt3Zr(0001) Model System to Powder Samples. *J. Mater. Chem. A* **2018**, *6* (36), 17587−17601.

(23) Korhonen, S. T.; Calatayud, M.; Krause, A. O. I. Stability of Hydroxylated (111) and (101) Surfaces of Monoclinic Zirconia: A Combined Study by DFT and Infrared Spectroscopy. *J. Phys. Chem. C* **2008**, *112* (16), 6469−6476.

(24) Danghyan, V.; Jaegers, N.; Pueyo, C. L.; Cain-Borgman, C. J.; Dellamorte, J.; Kundu, A.; Shangguan, J.; Iglesia, E. Lewis Acid Base Pairs as Highly Active Catalytic Sites for Hydrogenation and Dehydrogenation Processes. WO2024177986A2, 2023.

(25) Yaws, C. L. The Yaws Handbook of Physical Properties for Hydrocarbons and Chemicals. *Yaws Handb. Phys. Prop. Hydrocarb. Chem.* **2015**, 832.

(26) de Donder, T.; Van Rysselberghe, P. *Thermodynamic Theory of Affinity: A Book of Principles*; Stanford University Press, 1936.

(27) Van Rysselberghe, P. Consistency between Kinetics and Thermodynamics. *Chem. Eng. Sci.* **1967**, *22* (4), 706−707.

(28) Wei, J.; Zahner, J. C.; et al. Generalized Reciprocity Relation between Rates and Affinities of Simultaneous Chemical Reactions. *Ind. Eng. Chem. Fundam.* **1966**, *5* (1), 151−152.

(29) Dumesic, J. A. Analyses of Reaction Schemes Using De Donder Relations. *J. Catal.* **1999**, *185* (2), 496−505.

(30) Boudart, M. Some Applications of the Generalized De Donder Equation to Industrial Reactions. *Ind. Eng. Chem. Fundam.* **1986**, *25* (1), 70−75.

(31) Gounder, R.; Iglesia, E. Catalytic Hydrogenation of Alkenes on Acidic Zeolites: Mechanistic Connections to Monomolecular Alkane Dehydrogenation Reactions. *J. Catal.* **2011**, *277* (1), 36−45.

(32) Graham, J.; Rudham, R.; Rochester, C. H. Infrared Study of the Adsorption of Propene and Di-Isopropyl Ether on Rutile. *J. Chem. Soc. Faraday Trans. 1 Phys. Chem. Condens. Phases* **1984**, *80* (4), 895−903.

(33) Matyshak, V. A.; Sadykov, V. A.; Chernyshov, K. A.; Ross, J. In Situ FTIR Study of the Formation and Consumption Routes of Nitroorganic Complexes—Intermediates in Selective Catalytic Reduction of Nitrogen Oxides by Propene over Zirconia-Based Catalysts. *Catal. Today* **2009**, *145* (1−2), 152−162.

(34) Gabrienko, A. A.; Arzumanov, S. S.; Toktarev, A. V.; Stepanov, A. G. Solid-State NMR Characterization of the Structure of Intermediates Formed from Olefins on Metal Oxides (Al 2O 3 and Ga 2O 3). *J. Phys. Chem. C* **2012**, *116* (40), 21430−21438.

https://doi.org/10.1021/acscatal.5c04904
ACS Catal. 2025, 15, 19102−19110